



Deterioration of Israel's Caesarea Maritima's ancient harbor linked to repeated tsunami events identified in geophysical mapping of offshore stratigraphy



Beverly N. Goodman-Tchernov^{a,*}, James A. Austin Jr.^b

^a Charney School of Marine Sciences, University of Haifa, Israel

^b Jackson School of Geosciences, University of Texas, United States

ARTICLE INFO

Article history:

Received 25 April 2015

Received in revised form 19 June 2015

Accepted 23 June 2015

Available online xxxx

Keywords:

Tsunami

Geophysics

Sedimentology

Geoarchaeology

Harbors

Concrete structures

ABSTRACT

Modern observations have shown that harbors are especially vulnerable to the effects of tsunamis, both due to their position on the coastline and the tendency for tsunamigenic eddy production within enclosed harbor basins. Presumably, this was as much the case in the past as in the present. The Roman-era mega-harbor Caesarea Maritima, which is today submerged in some parts up to 5 m below sea level, is an ideal research site for understanding these impacts. Over the past three decades, archeologists, geologists and historians have searched for the cause of the rapid demise of this harbor, turning to explanations ranging from offshore faults, seismic disturbances, general failure and deterioration, to liquefaction and settling on unconsolidated sands. While tsunamis are recorded repeatedly in the Eastern Mediterranean historical record, it has only been in the past decade that physical evidence directly attributed to tsunamigenic sediments along the Israeli coastline near Caesarea has been documented. To date, deposits from at least three tsunami events that impacted the harbor have been identified in sediment cores, coastal exposures and archeological trenches, but no laterally continuous picture has been produced. In this study, using a dense offshore survey produced by a high-resolution subbottom profiler, shallowly buried sediment horizons offshore of Caesarea produce distinctive reflectors that correlate with the tsunamigenic stratigraphic sequence identified in cores and excavations. These surface structure maps allow for a laterally extensive reconstruction of these distinctive deposits. The results have led to the following conclusions and interpretations: 1) multiple offshore tsunamigenic horizons at Caesarea can be recognized, 2) individual tsunamigenic event horizons result in distinctive and unique surface morphologies that elucidate tsunami-based channeling/backflow processes, and 3) these backwash channels can be used to assess the general physical condition of the harbor at the time of each tsunami occurrence, ultimately revealing major differences between the state of the harbor following earlier events (i.e., 2nd c. CE) vs. later events (6–8th c. CE). We conclude that the combined acoustic-sampling approach is an effective way to document the interaction of tsunamis with harbor complexes/adjacent coastlines over millennia.

© 2015 Elsevier Ltd. All rights reserved.

1. Introduction and background

1.1. Evidence for tsunami impacts on coastal morphology and associated structures

Coastal morphology, including adjacent landforms, artificial structures, and coastal-fringing natural features (i.e., extensive coral reefs, mangroves, e.g., Baird et al., 2005; Fernando et al., 2005; Kunkel et al., 2006; Giri et al., 2008) can all influence the impact of tsunami wave flow (Hori et al., 2007; Sugawara et al., 2012). As the inundating wave breaches the coastline, natural and man-made obstacles that obstruct or impede the wave's force can lead to channeling and variable flow,

both as the wave advances inland and retreats seawards. Such energy redistribution is also evident in affected rivers or artificial channels, in which tsunami flow will continue inland to distances far exceeding that of uninterrupted portions of the coastline (e.g., Crete 1956, Bruins et al., 2008; Okal et al., 2009; northern Japan 2011, Mori et al., 2011; Goto, 2011a; Chile 2010, Fritz et al., 2011). The tsunami return/outflow is even more influenced by the presence of structures, and therefore is typically characterized by channeling (Umitsu et al., 2007; Feldens et al., 2009), which can result in shore-perpendicular bathymetric and topographic features (Atwater et al., 2010). In Sumatra following the 2004 tsunami, evidence of such complex back-flow included filled channels, boulders moved into deeper water, movement of sand into previously silty areas, and man-made rubble immediately seaward of the shoreline (Feldens et al., 2009; Goto, 2011b). Similarly, in northern Japan following the Tohoku-Oki earthquake in 2011, canals and road

* Corresponding author.

E-mail address: bgoodman@univ.haifa.ac.il (B.N. Goodman-Tchernov).

features often corresponded with variations in tsunami inundation heights along the Sendai Plain.

Amongst the range of coastal structures that interact with tsunamis, harbors have been identified as locations of acute magnification and flow intensification in both simulations and field studies (Raichlen, 1966; Synolakis and Okal, 2005; Lynett et al., 2012). For example, during the 2004 tsunami, at the Port of Salalah, Oman, strong currents produced inside the harbor caused a 285 m ship to break away from its moorings and beach on a nearby sandbar after spinning and drifting for hours (Okal et al., 2006). At Port Blair, India, harbor structure damage included movement or complete collapse of the jetties (Kaushik and Jain, 2007). Examples are also available for the far-field effects of tsunamis, where harbors have been damaged while adjacent coastlines experience little inundation. One such harbor is located in Crescent City, CA; this site was damaged repeatedly following both near-field events, such as Alaska 1964, as well as far-field tsunamis, such as those generated from seismic events in 2006 (Kuril Islands) and in 2011 (Tohoku-Oki) (Griffin, 1984; Horrillo et al., 2008; Kowalik et al., 2008; Wilson et al., 2013). Widespread documentation of ships originally moored in harbors that have been displaced inland and/or damaged along the adjacent coastline during tsunamis are common; this phenomenon includes relatively small events, such as the tsunami following the 1999 Izmit earthquake in Turkey, with varying reports of wave heights, but with possible localized heights of ~6 m (Rothaus et al., 2004).

Following a tsunami, a variety of characteristic markers can be left behind, both on the shallow sea bottom and on shore, including massive debris fields, sheets of sand, muddy film, and/or eroded surfaces, amongst a list of over thirty-two published indicators (e.g., Goff et al., 2012). Depending on the specific surface conditions of the impacted coastline, e.g., surficial sediment types, strandline morphology and available unconsolidated debris, coastal zone bathymetry can be altered as contents carried within the tsunami flow drop out as the wave energy dissipates (Jaffe et al., 2012). Inland, tsunami-based deposits are generally characterized by landward thinning (Morton et al., 2007), unless interrupted by some limiting structure or topography.

The patterns of tsunami deposits and bathymetric forms created by these waves can be informative regarding the character of the affected coastline and adjacent offshore areas (Richmond et al., 2012). In northern Japan, for example, artificial channels and a highway constructed on the Sendai Plain before the 2011 Tohoku-Oki earthquake influenced the distribution of tsunami-deposited sediments and wave run-up heights (Sugawara et al., 2012), relative to the distribution of known preexisting tsunami deposits. Recognizing and mapping tsunami-related features from historical events should inform us as to the state of both natural and artificial structures on a coastline which were affected by these tsunamis, including the influences of the back-wash phase of sedimentation. In this study, the ancient harbor of Caesarea Maritima, on the eastern Mediterranean coast of Israel (Fig. 1), is presented as an ideal site to consider this tsunami-impact phenomenon, and how and whether the physical evidence for such recurring impacts might be preserved over two millennia.

1.2. Caesarea Maritima: the ancient harbor, its deterioration and demise, and recent tsunami research

When King Herod had the city of Caesarea built on the coastline of what is now Israel between 25 BCE and 9/10 BCE, he applied Roman city planning, organization and building techniques, including the costly installation of a state-of-the-art, artificial mega-harbor (Holum et al., 1988; Hohlfelder, 1988, 1996; Raban, 2009; Votruba, 2007; Raban, 2008; Fig. 1). The natural environment afforded little protection or anchorage, with the exception of periodic, remnant, exposed ridges of eoleonite sandstone (locally referred to as 'kurkar') roughly paralleling the coastline immediately offshore. These bedrock structures are exposed and eroded lithified dunes 135,000–45,000 year old (Sivan and Porat, 2004). The harbor was constructed on portions of this bedrock and extended seaward onto unconsolidated Nile River-derived sands (Goldsmith and Golik,

1980; Neev et al., 1987; Stanley, 1989; Zviely et al., 2007), with the use of man-made foundations. Roman engineers succeeded in this task by building wooden frameworks ('caissons') on land, then towing them into position where they were submerged, filling them with hydraulic cement, and ultimately finishing them with above-water superstructures. Fields of large cobbles (<20 cm diameter) were emplaced beneath the caissons (Raban, 2008), presumably to give them added stability against erosion and undermining, suggesting that the engineers of the time were aware of the inherent risks for constructing directly on unconsolidated sandy sediments. These caissons were arranged in rows to produce the spinal walls of the harbor, completing the entire project in <15 years (Brandon, 1996). This efficient approach to harbor construction continues to be used today. For example, 'Mulberry I' and "Mulberry II", created by the allies during WWII in preparation for the D-Day landings, were also artificial islands constructed in a similar manner for the purpose of providing supplies and reinforcements until an established harbor could be secured (Stanford, 1951; Ryan, 1959; Bettwy, 2015).

Descriptions made ~70 CE by historian Flavius Josephus describe a fully functional imperial mega-harbor, exceeding the size of most contemporaneous Mediterranean harbors (Raban, 2008). Josephus explicitly describes the expense of and investment made in the harbor's construction. Excavations have since supported these grandiose statements, revealing bulk raw building materials that traveled long journeys before arriving in Caesarea (Votruba, 2007). For example, chemical analysis of the volcanic ash ('pozzolana') used for producing the fast-drying hydraulic cement shows that the ash was brought from Vesuvius (Brandon, 1996; Hohlfelder et al., 2007), while the underlying cobble and rubble beds beneath the cement-filled caissons show non-local mineralogies common to Turkey, Cyprus, and parts of Greece. The wood used for the caisson frames, as was common practice in shipbuilding practices of the time, came from the cedar forests of Lebanon (Votruba, 2007).

However, despite the significant investment and durability of the cement used in the construction process (Jackson et al., 2012), the overall state of the harbor had significantly deteriorated by the end of the 2nd century CE, and probably even earlier, according to radiocarbon-dated sedimentological evidence showing a shift from a low-energy, harbor environment to an open-water exposed, unprotected environment during that period (Reinhardt and Raban, 1999; Reinhardt et al., 1994). Throughout the 1990s, the generally accepted presumption arising from these studies was that the harbor experienced its demise due to some combination of earthquake-related liquefaction, with some credence also given to the possibility of related tsunami, though without clear markers then to support such a hypothesis.

Caesarea harbor phases, from initial construction to the present, have been reconstructed using sedimentological, geophysical (i.e., magnetometry), and archeological surveys (Reinhardt et al., 1994; Reinhardt and Raban, 1999, 2008; Boyce et al., 2009). The most recent summary (Reinhardt and Raban, 2008) suggests six such phases, summarized as follows: 1) initial construction, 1st century CE, 2) 1–2nd century CE destruction, 3) 3–4th century CE, unprotected (meaning exposed to the open sea and therefore without intact harbor features), 4) 4–6th century CE, natural/unimproved harbor, 5) 6th century CE, sand infilling, and 6) 6–11th century CE, renovation/destruction. Unfortunately, the foregoing summary remains vague regarding causation, as it predates later findings (Goodman-Tchernov et al., 2009) that bring to light evidence for tsunami events in both the Byzantine (4–6th c. CE) and Early Islamic (7th–8th c. CE) periods, as well as confirming an earlier suggestion of another 2nd century CE wave-based event (Reinhardt et al., 2006).

Previous geophysical research on the Caesarea Maritima harbor has included both seismic and magnetic surveys (Mart and Peregman, 1996; Boyce et al., 2004, 2009). Boyce et al. (2004) conducted a magnetic survey with the aim of determining the feasibility of using magnetic signatures to map and define the concrete installations of the harbor, as the pozzolana cement used by the Romans was iron-rich. Although the high resistivity of the kurkar bedrock proved to be challenging, the overall form of the foundations of the harbor, particularly the individual

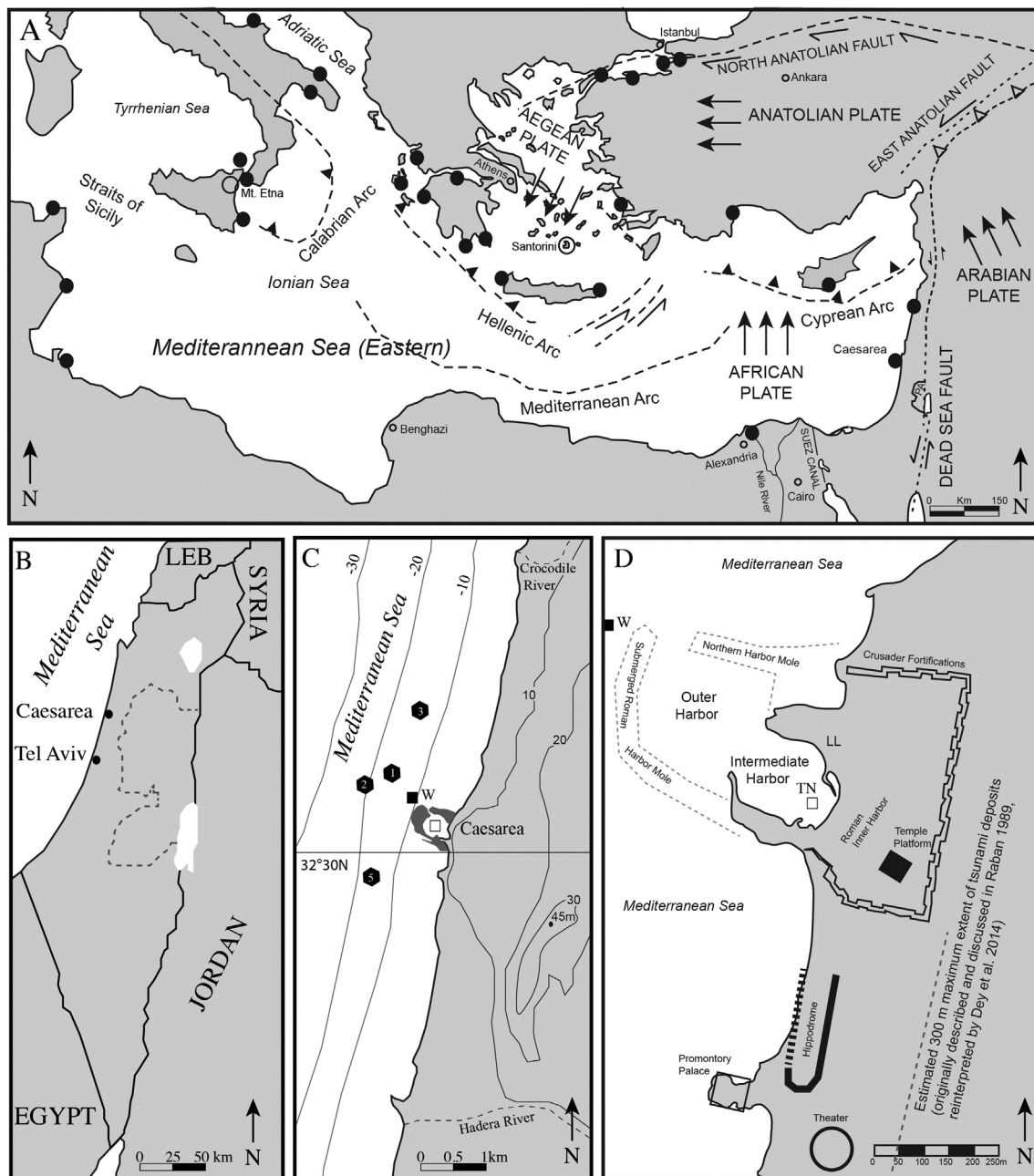


Fig. 1. A) Map of eastern Mediterranean Sea with major tectonic and volcanic features highlighted. Circles represent volcanoes discussed in the text and filled circles represent locations in which tsunamigenic deposits have been documented in this region (adapted from summary of Vött, 2011). B) Study site in context of neighboring countries. C) Local features near site. Empty square within the harbor moles represents the area of inner harbor shallow excavation areas 'TN' and 'TNZ'. Topography in meters. For further description of excavation results and stratigraphic sequence, see Reinhardt and Raban (2008). D) Harbor areas of Caesarea with features mentioned in text highlighted.

caisson forms, was discernable. Due to the significant difference between the near-coastal harbor features, which remain at their correct elevation relative to sea level, and offshore harbor features, which are now submerged up to 5 m depth, earlier work had suggested that movement along a shore-parallel fault, which became active following construction of the harbor, could be responsible for the modern elevation change (Mart and Perecman, 1996). As a result, for many years afterward, theoretical north–south trending fault lines remained on maps of Caesarea. However, after failed attempts to recognize these features in the field through additional geophysical mapping, along with jetprobe surveys of the sediments with associated seafloor excavations (Raban, 2008), such structures are now rarely included. Instead, the observed coast-parallel offset in elevation is now presumed to relate more directly to the classic challenges faced when constructing directly on

bedrock versus adjacent (offshore) unconsolidated sediments. Areas of the harbor constructed seaward of the firm kurkar bedrock foundation were likely more susceptible to liquefaction, undercutting, scouring and erosion, promoting subsidence of harbor features farther offshore, whether by storms, earthquakes, or tsunamis.

Historical evidence for tsunamis in the eastern Mediterranean supports a minimum of 21 events, three referring to the city of Caesarea directly (115 CE, 551 CE and 1202 CE; Shalem, 1956; Amiran et al., 1994). Archeologists have been aware of these events for decades (see discussion in Dey et al., 2014), but they have lacked the comparative tools or reference data to ascribe particular deposits (onshore or offshore) to tsunami-derived causes. As a result, alternative explanations for these seemingly anomalous deposits found in archeological sites have been put forward. For example, laterally extensive shell beds encountered

in terrestrial excavations in Caesarea, which could be evidence tsunamigenic origin, have been previously ascribed to be the result either of dredging activities or as construction fill (Neev and Emery, 1989). Tsunami sedimentological research has also advanced, particularly in response to the destructive tsunamis of Sumatra 2004, Java 2009, Chile 2010 and Tohoku-Oki 2011 (e.g., Szczuciński, 2011; Goff et al., 2012; Pilarczyk and Reinhardt, 2012; Pilarczyk et al., 2012; Goto et al., 2014). As a result, there is now an extensive, robust body of comparative data for interpreting and understanding historical, pre-historical and paleo-tsunamigenic deposits (e.g., Bourgeois et al., 1988; Goff et al., 2012), which did not exist a decade ago.

This increase in knowledge has led to the recognition of more such tsunamigenic deposits worldwide, both in the archeological and geological records (e.g., Pareschi et al., 2007; Vött et al., 2009; de Martini et al., 2010; Yawsangratt et al., 2011; Marco et al., 2014, but see also criticism of this approach in Galili et al., 2008; Morhange et al., 2014). However, despite this increased awareness, the number of tsunamigenic sedimentological deposits documented from the Levantine Sea region, and other parts of the Eastern Mediterranean, still only begins to approach the number of events recorded in the written record (Papadopoulos et al., 2014), suggesting that discovery of these deposits in this historically important part of the world remains incomplete.

Research on the demise of Caesarea's harbor (Reinhardt et al., 1994; Reinhardt and Raban, 1999) agrees generally that the timing of initial major deterioration had occurred *at least* by the end of the 2nd century CE (see also Raban, 1992; Raban, 1995; Reinhardt and Raban, 2008; see Hohlfelder, 2000, for alternate timing). Evidence to support the role of tsunamis in this initial damage takes the form of laterally extensive sedimentary horizons with interpreted tsunamigenic characteristics (details follow below) recorded offshore, as well as reviews of archeological reports demonstrating the presence of corresponding deposits on land (Reinhardt et al., 2006; Goodman-Tchernov et al., 2009; Dey and Goodman-Tchernov, 2010; Dey et al., 2014).

Reinhardt et al. (2006) have characterized a tsunami deposit, found in an excavation trench (Area 'W', see Fig. 1C) outside of the ancient harbor, based on the presence of imbricated allochthonous shells (predominately *Glycymeris violescens*), with radiometric ages (1st c. BCE to 2nd c. CE) corresponding with a historically documented tsunami event at 115 CE (Shalem, 1956). Other defining characteristics of this deposit include an erosional basal contact, and mixing of included clast sizes. Goodman-Tchernov et al. (2009) have also investigated the lateral extent of this reported horizon, and identified its continuation, as well as the presence of additional interpreted but distinct tsunami horizons, based on the same criteria and an additional seven tsunami-related indicators: micropaleontological assemblage, fining upward sequence, tilted marine installations, larger standard deviation of particle size distributions (relative to typical background), out-of-place household items, rip-up harbor mud clasts, and rafted terrestrial organic material. Reports from terrestrial archeological excavation reports pre-dating the Reinhardt et al. (2006) initial recognition of these tsunami deposits were also revisited by Goodman-Tchernov et al. (2009) to determine whether other horizons containing possible tsunami-related inclusions had been described in the literature but not interpreted as such. Their realization was that a wide range of distinctive stratigraphic evidence for tsunami-related deposits was present. Other sorts of interpretations had included construction fill or dredging refuse dump, but these were refuted in light of new tsunami characterizations (Dey and Goodman, 2010; Dey et al., 2014). In this paper, regional high-resolution seismic profiling offshore the harbor mouth of Caesarea is combined with ongoing marine archeological investigations to show the regional impact of multiple tsunamis on both this harbor and the adjacent coastline over the past two millennia.

1.3. Offshore tsunami deposits

Generally speaking, the near offshore environment has not been heavily mined for tsunami evidence. While tsunami-related studies

have increased exponentially in the past decade, there are far fewer studies that present shallow offshore finds. In their summary of the state of research in paleotsunami deposits Rhodes et al. (2006) asked, "Does a record of paleotsunamis exist in the near offshore stratigraphic record?". By that time, Vandenberg et al. (2003) had demonstrated the presence of shallow offshore deposits using both geophysical survey and coring in NW Java, Indonesia and Abrantes et al. (2005) described events correlatable to sediment core horizons in Lisbon, Portugal. Since then, a few studies of past and recent tsunami events and modeling have answered Rhodes' question in the affirmative as well. Some examples beyond the work in Caesarea (Reinhardt et al., 2006; Goodman-Tchernov et al., 2009; Dey and Goodman 2010; Dey et al., 2014) include cores collected from Augusta Bay, Italy (de Martini et al., 2010; Smedile et al., 2012), offshore boulders mapped in western Banda Aceh, Indonesia (Paris et al. 2009), Weiss and Bahlburg's (2006) modeling predictions suggesting the presence of deposits in the shallow offshore. The near offshore environment is still more poorly understood relative to terrestrial coastal areas.

2. Methods

A seismic survey was carried out offshore Caesarea using a portable Knudsen 320 BP CHIRP (2.5–5.5 kHz) profiler mounted on a ~8 m long catamaran workboat. A dense grid (~5 m average profile spacing) was collected both along-strike and across strike, with a total track length of ~126 km (Fig. 2). A GPS navigation antenna mounted directly over the CHIRP transducer determined position. The survey area covers the outer portion of the ancient harbor, and also includes positions of previously published excavation trenches and sediment cores (Fig. 2). Minimum water depth of the survey was ~3 m within the ancient harbor area, while the maximum was ~10–15 m farther offshore. Survey lines were collected during the calmest hours of the day (early morning to mid-day) to minimize the effects of wave disturbance, and then smoothed/compensated for vessel heave during post-processing. After collection and post-processing, which included band-pass filtering as well as heave compensation, the seismic data were interpreted in travel-time by identifying and 'picking' continuous reflectors, using the Landmark Decision Space® seismic interpretation software package available at the University of Texas Institute for Geophysics (UTIG).

Reflector depths have been inferred from the travel-time maps using a constant sound velocity of 1.5 km/s. The velocity was selected because it is a typical compressional wave velocity for water. For this study, it was considered the most reasonable number to use in the absence of direct measurements of the velocity in the cored sediments. As a result, a 5–10% underestimation of depths to the sub-seafloor reflectors may exist, as typical velocities in surficial sediments are generally in the 1.55–1.7 km/s range. Then, identified and mapped reflectors have been compared to previously described horizons identified from sediment cores within the survey area, to determine the geologic identity of reflectors ('ground truth'), and to extrapolate the morphological details (bathymetric expression) of the horizons laterally across the study area. Prominent reflectors interpreted and mapped within the survey area were then compared to the stratigraphic sequences, ages and depths identified from previous excavations and sediment cores.

3. Results and interpretation

3.1. Seismic reflectors and sedimentological correlation

Sub-seafloor penetrations up to ~4–5 m were achieved, with particularly in deeper water (Fig. 3); multiple sub-bottom horizons can be identified and mapped over much of the surveyed area. However, sub-bottom penetration is spatially variable in these sand-prone sediments; correlation difficulties relate both to the uneven acoustic penetration as well as the presence offshore of "kurkar" ridges, the aeolinite sandstone ridges approximately paralleling the modern shoreline that represent

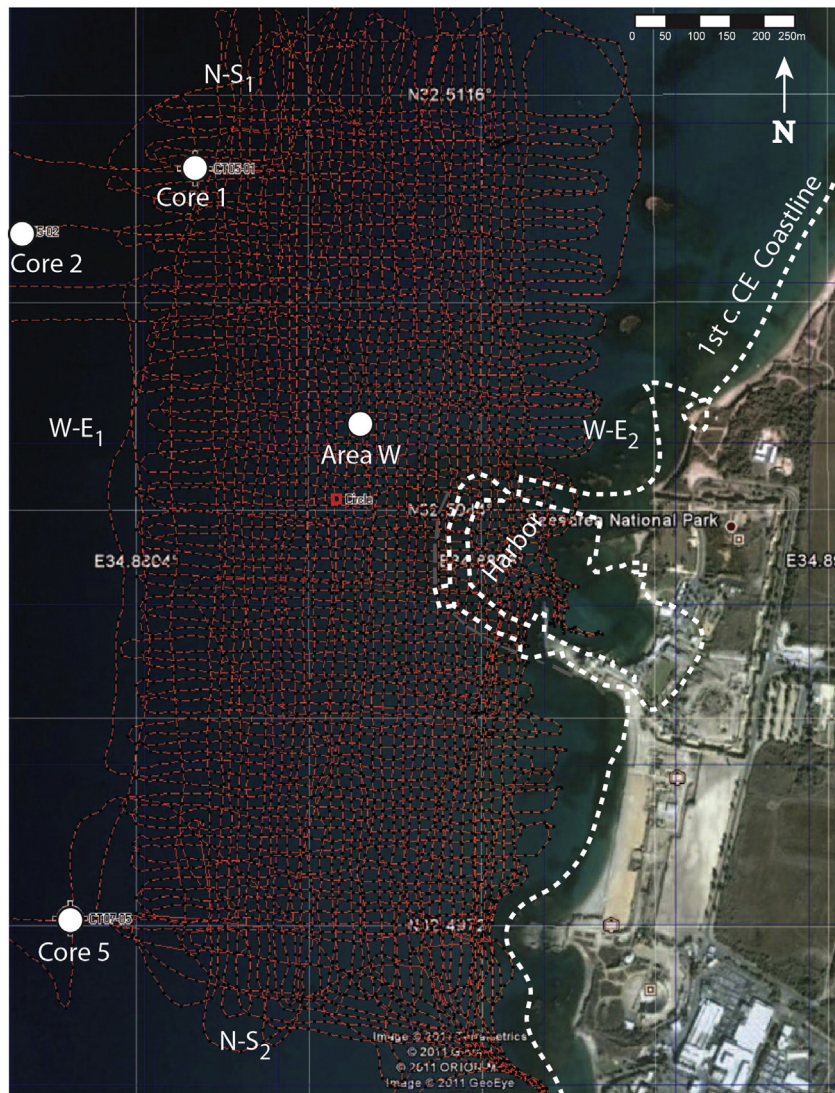


Fig. 2. CHIRP profiles (red dashed lines), collected offshore of Caesarea in August 2011. Total track length was ~126 km, and profile spacing was ~5 m. Each dip profile is ~0.65 km long, while each strike profile is ~1.4 km long. Note locations of cores/seafloor excavations (red square, white dots), within which tsunamites were interpreted (Goodman-Tchernov et al., 2009). Remains of the ancient Roman city lie to the east; part of the ancient harbor still exists, defined by the remains of semi-circular moles/groins visible just below “Caesarea National Park” in this satellite image. The approximate outline of the original harbor is shown (white dashed lines). White arrowheads denote the locations of the strike and dip profiles shown in Fig. 3.

now-submerged Pleistocene dune complexes (Fig. 3A). These ancient lithified dunes produce physical barriers that both alter the depositional regime as well as complicate sub-seafloor geophysical mapping.

Despite these limitations, in addition to the surface bathymetry, two reflectors (‘A’ and ‘B’) were mapped across the entire survey (Fig. 3). In some sections, a deeper, third reflector (‘C’) residing in topographic lows in the acoustic basement formed by the kurkar ridge complex is also evident, but this reflecting horizon cannot be mapped everywhere (Fig. 3A). The acoustic basement cannot be followed throughout the survey area as a combined result of the topographic complexities of the kurkar ridge complex and the limited penetration capability of the small, portable CHIRP system used (Fig. 3B). Reflector C was mostly absent in depths below 10 masl.

When comparing the reflectors to cores taken within the survey area, the mapped reflectors ‘A’ and ‘B’ correlate approximately in depth with three possible tsunami horizons (Fig. 4), though the upper two horizons are selected for association. This interpretation is based on three primary arguments: 1) where overlap occurs with the cores in deeper water, these horizons are better correlated to the upper two horizons when compared to depth, which can then be extrapolated into the shallower depths, 2) previous sedimentological research

suggests that, generally, there is less preservation of the oldest/Santorini event relative to later events, especially in shallower conditions (1 to <12 m water depths, Goodman-Tchernov et al., 2009), and 3) where a purported Santorini-age horizon is preserved, sedimentological indicators suggestive of its being a tsunamite can sometimes be less clear, due to a dearth of anthropogenic inclusions, as the harbor city did not yet exist, and a lack of physical properties conducive to producing a seismic reflection (Goodman-Tchernov et al., 2009).

The detailed sedimentological description of these reflecting horizons (Fig. 5), and associating it to radiocarbon-dated samples at the same sub-seafloor depths, suggests that horizons “A” and “B” correspond to the two most recent tsunamigenic deposits recovered in available cores (Fig. 4). The coarse, clastic nature of these tsunamigenic deposits is likely to exhibit a significant acoustic impedance contrast. Furthermore, these shallower horizons are more likely to have a higher degree of preservation generally than the older/deeper ‘Santorini’ deposit, which coincides with a tsunami that occurred as a result of the Thera volcanic eruption at ~1620 BCE (Friedrich et al., 2006, “Reflector C”). These layers (Fig. 5) include larger amounts of man-made materials (pottery) and freshly transported as well as reworked shell fragments; therefore resultant higher densities will result in clear, mappable

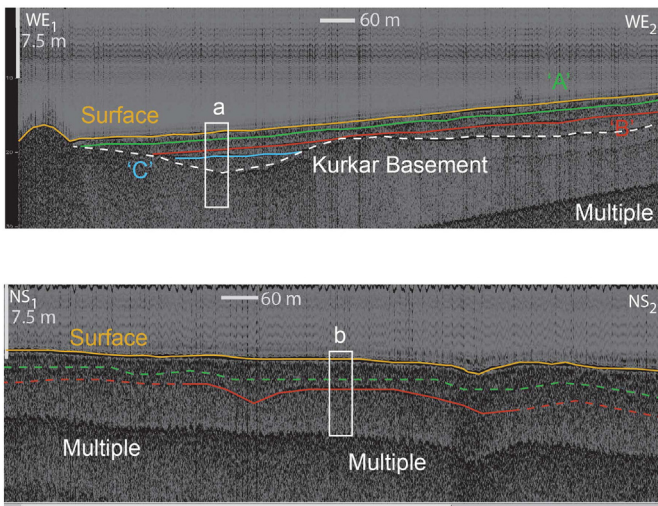


Fig. 3. A. Portion of a dip-oriented CHIRP profile ('WE') from the 2011 survey offshore of Caesarea (see Fig. 2 for location). Profiles were collected in travel-time; actual depth in meters is an estimate using water velocity. Both the seafloor (orange) and the seafloor multiple are labeled. Two prominent sub-seafloor reflectors ("A" and "B") can be observed at variable depths up to a few meters below the seafloor, and may relate to tsunamites identified by Goodman-Tchernov et al. (2009). A "third" prominent, even deeper intrasedimentary reflector ("C") is observed on this profile, but could not be mapped throughout the survey area. Note the kurkar ridge bounding this profile on its seaward side; these kurkar ridges/lithified paleo-dunes form acoustic basement in the survey area. A landward subsurface continuation of this ridge complex may be observed in a couple of places, but these ridges could not be mapped continuously in the subsurface. B. Portion of a strike-oriented CHIRP profile ('NS') from the 2011 survey (see Fig. 2 for location). The uninterpreted profile is shown in the small inset (top left). Profiles were collected in travel-time; actual depth in meters is an estimate using water velocity. Both the seafloor (orange) and the seafloor multiple are labeled. A prominent reflector ("B", in red) can be observed at variable depths up to a few meters below the seafloor. Reflector "A" (dashed green line) is only tentatively identified on this profile. The reflectors were picked based on their visual lateral continuity and logical spatial continuation patterns. This is in part linked to amplitude information, but is also an interpretive skill gained with experience that has some subjective bias.

reflectors like "A" and "B", as were observed (Fig. 3). Furthermore, the available sediment record suggests a period of tsunamite quiescence (>1500 years, Fig. 4) at Caesarea following the Santorini-age event. The data suggests that this long time interval may have also allowed more time for alteration and erosion to obscure the Santorini tsunamite, particularly in the shallow, storm exposed depths. For example, the Santorini-age event is missing beneath the 1–2nd century event horizon in Area W where there is a 3000-year disconformity (Fig. 4, also see Reinhardt et al., 2006); where our dip profile crosses that area, the presumably correlative reflector "C" also does not occur (Reinhardt et al., 2006; see also Fig. 3A). No Santorini event can be discerned across much of the shallow water (<8 masl) area (Reinhardt and Raban, 2008; 3A). This missing horizon, suggests that at least 1700 years (from ~1600 BCE to 115 CE) of accumulated sediments were removed as a result of the December 13, 115 CE tsunami recorded in the historical record (Reinhardt et al., 2006). The data shows that the non-continuous reflector 'C', that is observed only in lows within the underlying acoustic basement topography, relates to preserved portions of the Santorini event. Such selective preservation was likely the result of localized effects, such as concentrations of shells in topographic lows. Given that one of the most conservative indicators used for the identification of all tsunamigenic events at all depths offshore Caesarea is increased standard deviation (i.e., poorer sorting) values of particle-size distribution <2 mm (Fig. 5), then the Santorini event is only producing a reflector when it is preserved and contains high shell content.

3.2. Top plan surface morphology (paleo-bathymetry) of reflectors

After identification and interpretation, the surface and underlying reflectors were isolated and used to produce independent surface contour maps of the modern seafloor and horizons A and B (Fig. 6). It was presumed that if the mapped subsurface reflectors are a record of gradual or typical background sedimentary events, then it is anticipated that their surface morphological surfaces would have some consistency from reflector to reflector; responding more to the inherited underlying

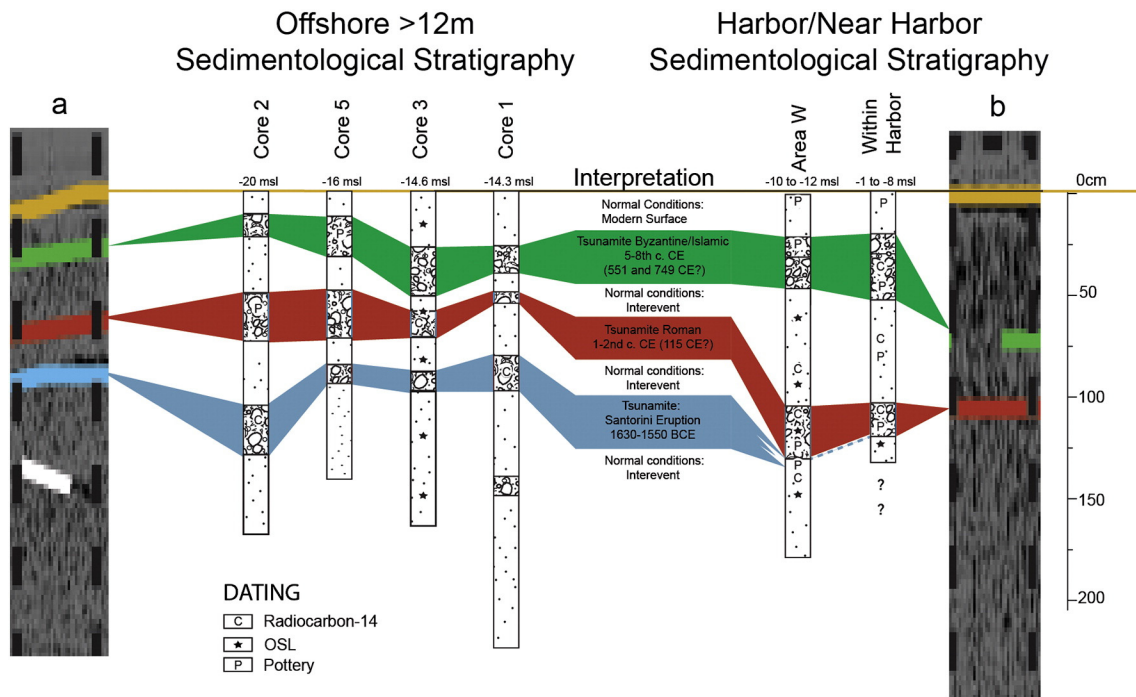


Fig. 4. Dip and strike CHIRP profiles (see Fig. 3), from which sample segments "a" and "b" have been enlarged for comparison with previously identified sediment core and underwater excavation stratigraphic compilations within the surveyed area (Reinhardt et al., 2006; Reinhardt and Raban, 2008; Goodman-Tchernov et al., 2009). Three horizons, representing four tsunami events, are recognizable from the available core evidence within the surveyed area (for core locations, see Fig. 1C).

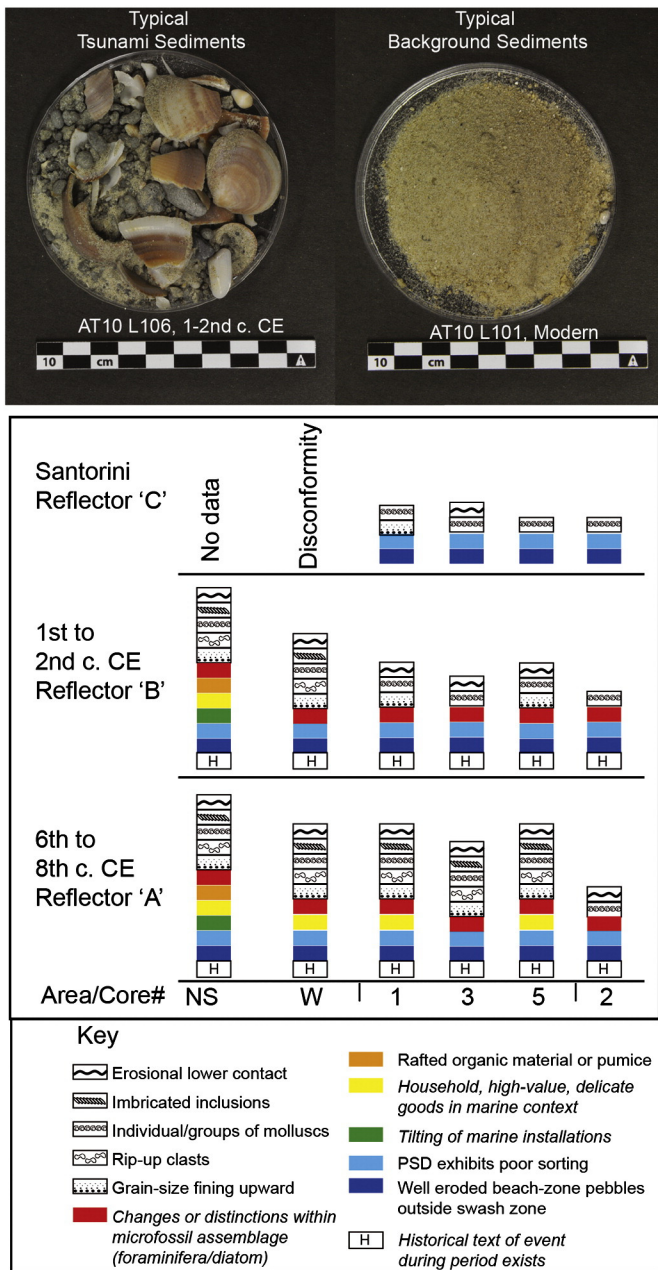


Fig. 5. Sediment characteristics of several of the presumed “tsunamiites” sampled offshore Caesarea. Upper photographs demonstrate tsunamigenic (left) and background sediments (right). Note how coarse-grained the interpreted tsunami-based sediments are, such coarse, poorly-sorted sediments would be highly reflective. Lower illustration summarizes characteristics that have been found in tsunamigenic horizons from onshore to offshore, highlighting the decreasing number of indicators with greater distance offshore. Indicators that are expected only after construction of the harbor (i.e., not present at time of Santorini eruption-aged event, see Fig. 4) are italicized in key. For locations of cores, see Fig. 1C.

coastal bathymetry and/or artificial features present at the time they were created. However, if the morphologies of each layer show unique distinction from one another, it would suggest some added influence, possibly variations in the coastal features or other geomorphological changes. These three morphology compilations were used to determine whether these surfaces preserve features, and whether they resemble those described following tsunami events, like channeling caused by run-up and backwash, or whether indications of changes and modifications in artificial man-made features on the adjacent coastline (i.e., evolution of the harbor shape and size over time; Fig. 6) are present and associated to these features to assess the impacts of tsunamis on the Caesarea coastline through time.

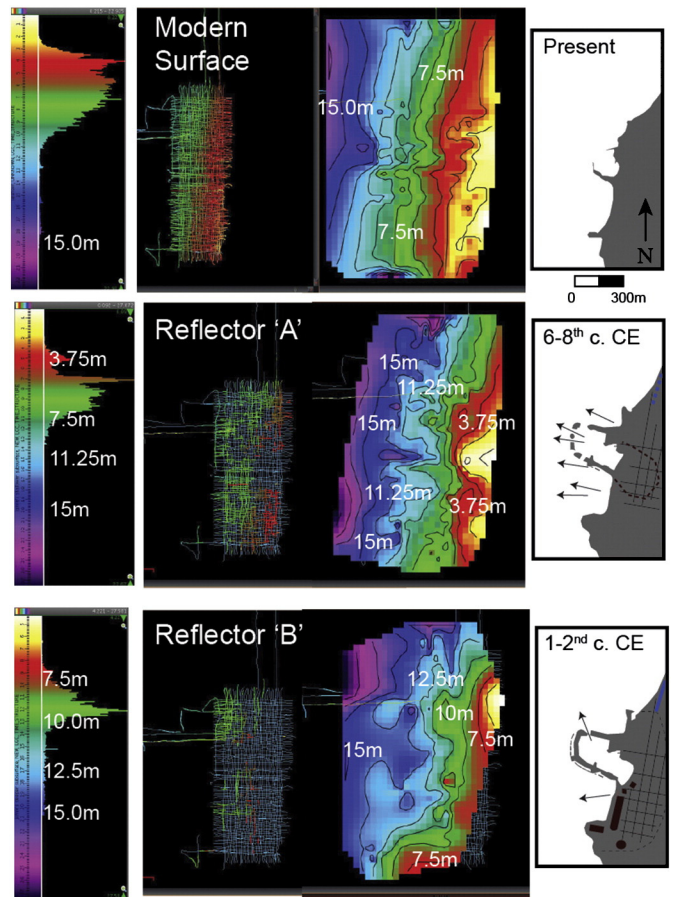


Fig. 6. Structure maps of A.) the modern seafloor, B.) reflector “A” (see also Fig. 3), and C.) reflector “B” (see also Fig. 3). To the right of each structure map, using observed channels in each map as a guide, we hypothesize tsunami-based outflow directions from the Caesarea harbor as it existed morphologically at three different time: ~1st–2nd century CE (115 CE), 6th–8th century CE (551/749 CE), and the present. For details, see the text. The modern bathymetry reflects submerged harbor and coastal kurkar features. Major intact coastal features include Crusader-era city walls and moat. The 6–8th century A.D. (551 CE, 749 CE) “A” horizon includes multiple drainage-like features that are distributed more evenly along the coastline, which we suggest is a lack of a cohesive single harbor entrance and fewer monumental coastal structures. The horizon “B” structure map includes one or two pronounced channels, concentrated at the mouth of ancient harbor. We conclude that these features indicate focused backchanneling at the harbor entrance, with possibly an additional focal point on the southern side of harbor (possible association to sluice channels described by Raban (1992)).

3.2.1. The modern bathymetry

Today, there are no running rivers in the immediate vicinity of Caesarea; the closest flowing rivers are ~2 km to the north and south (Crocodile and Hadera rivers). Nonetheless, both coast-normal and coast-parallel topographic variations can be observed in the mapped bathymetry (Fig. 6A), that coincide to both harbor features and kurkar ridges, respectively. The observed complexity is likely a combined result of incompletely buried submerged harbor structures known from excavations and previous geophysical mapping (e.g., moles, groins; Boyce et al., 2004) and exposed kurkar ridges/bedrock seaward of the coastline. However, no substantive onshore–offshore drainage features or channeling are present.

3.2.2. Reflector ‘A’: Late Byzantine/early Islamic periods (tsunami events at 551 and 749 CE)

The map of the shallow reflector surface “A” (Fig.6B) looks very different from the modern seafloor, although this subsurface horizon is only buried <1 m deep. Sub-parallel channels extend from near the coastline, beginning in water depths of ~8–9 m, and to water depths

of at least ~15 m. Data shows at least three of these onshore–offshore drainage systems, and there may be as many as six. This mapped topography and in particular the presence of the distributed observed onshore–offshore channels from south to north, suggests that a series of coastal features interrupted the backflow stage of the tsunami that are tied sedimentologically to this reflecting horizon (Fig. 4).

3.2.3. Reflector 'B': Roman Period (tsunami at 1–2nd c. CE, possibly 115 CE)

The map of reflector "B" (Fig. 6C) shows a minimum of one, and possibly two channel systems, with one complex, dendritic feature situated roughly offshore of the modern harbor mouth, and another ~N–S oriented channel in the northernmost part of the survey area. The central drainage feature begins in water depths of ~8–9 m, and extends outward to the western limit of the surveyed area in water depth of ~15 m. This surface occasionally onlaps buried kurkar ridges offshore (Fig. 3A).

4. Discussion

The interpretation of three sub-seafloor reflectors mapped offshore of Caesarea (Fig. 3) conclude with the presence of distinctive and unique coastal structural configurations at the time of past tsunami events. The mapping suggests regionally significant impedance contrasts, that were interpreted here as marking the last/uppermost expression of known tsunami deposits previously sampled, analyzed and interpreted on this margin (Fig. 4). In all cases, we assume, and this is supported by modern studies elsewhere (Paris et al., 2009), that immediately following any tsunami, complex processes of alteration and erosion occur, particularly in depths exposed to storm activity and other coastal processes (e.g., long shore transport). In this part of the Mediterranean, these tsunami deposits, or what part of them is preserved after exposure to later storm and long-shore transport effects, are buried under Nile River-derived sands. Therefore, we suspect that the reflector maps of the two subsurface reflectors (Fig. 6B, C) does not give a reading of what the sea bottom looked like *immediately* following the tsunami, but at the time of the tsunami deposit's eventual burial, which could be a matter of decades or more. Therefore, the apparent drainage features we observe are probably only preserved remnants of tsunami backwash features which, at the time of their formation, would have been even more distinctive and pronounced, as is true in modern analogues (Bahlburg and Spiske, 2012; Feldens et al., 2009; Hori et al., 2007; Paris et al., 2009). Each event has a unique signature that relates to the state of the coastline and the structures present at that time.

The deepest reflector, 'C' (Fig. 3B), which is associated here with what is left of the Santorini-age tsunamite, is not sufficiently preserved offshore Caesarea to identify except in topographic lows in the kurkar topography (Fig. 3B), and in deeper water. The unaltered coastline in this area is high-energy, with little natural protection, which is one of the reasons that specialized engineering methods were required to create the Caesarea harbor. Therefore, prior to the harbor's construction, at the time of the Santorini-age event (Fig. 4), tsunami deposits in shallow water would not have had a good chance for preservation due to their exposure to the open sea, but were more likely redistributed and transported during storms; we also see such storm-related redistribution today. In contrast, later events following the construction of the harbor have a greater chance of preserving due to the more protected nature within the harbor area, even if only in relative terms, from the full force of incoming storms. This is observable today during storms in which the waves are noticeably attenuated within the semi-protected harbor bay, despite the harbor's generally dilapidated condition. Sedimentological evidence clearly shows the presence of the Santorini horizon in water depths > 10 m (Fig. 4). In area 'W' (Fig. 1C; 4, upper right) the stratigraphic sequence includes a major hiatus (~3 kyr of missing sediment), which includes the level at which the Santorini horizon would have been expected. We expect such a hiatus in area W, as it is located just outside the harbor entrance, and would have experienced

focused outgoing flow capable of substantial erosion and scouring during the back-channeling phase of a tsunami. In addition, because harbors are known to intensify the effects of tsunamis, any Santorini-aged tsunami deposits in shallow water that survived until the construction of the harbor would have been vulnerable to further erasure following the first of the post-harbor construction tsunami events (Fig. 4).

Reflector B's surface morphology includes a main channel complex that corresponds approximately with the position of the harbor entrance (Fig. 6C). Because Caesarea's harbor is believed to have been in good condition at the time of the 2nd century tsunami, the incoming wave must have encountered an intact and standing outer harbor mole, which would have forced abrupt shoaling of the incoming wave, scouring deeply the area immediately outside the harbor, while also breaching the tops of man-made features. Incoming wave inundation must also have run up within the harbor, as well as along the coastline north and south. However, during subsequent retreat of the wave, that outflowing water would have concentrated through the harbor mouth, between the reinforced moles (Fig. 2), preferentially scouring and eroding the region immediately outside the harbor entrance and depositing larger deposits farther offshore, as is evident in the ~80 cm 2nd century deposit in Area W (Reinhardt et al., 2006). Estimating the velocity of the flow exiting the harbor mouth during the 115 CE event is possible, because archeological evidence exists for the movement and toppling of an artificial island that stood at the harbor entrance at that time (Raban, 2008). During excavations there in the late 1990s, concrete was exposed and a vertical contact between cement layers of different fabrics was recorded. These cement layers are a remnant of the construction process, during which different cement mixes were used at different phases of filling the wooden caissons (Brandon, 1996; Hohfelder et al., 2007). At the time of construction, after the cement cured, the different concretes layers lay horizontal upon one another; therefore, any shift from the original position at construction can be identified due to the offset of that horizontal contact. In the case of the tower, the near-vertical contact indicates at least a 90° shift of the caisson after the harbor was completed. It was also observed that no wood was preserved on any outer surface of the island, whereas typically protected, unexposed sides of the caissons included some preserved wood, again suggesting that all sides of the island, which was essentially once a wood-faced concrete cube, had been exposed on all sides fully to the elements at some point of time, a situation only possible with the turning of the caisson. Artifacts found around the base of the toppled tower post-date the 1st century CE, with the earliest coin found aged at 144 CE. These deposits are not beneath the tower, but rather along the edges of the tower within the typical scouring areas where debris is regularly trapped in harbor entrances. Excavations did not tunnel fully below the towers due to safety concerns. Such artifacts might provide an age maximum for the timing of the tower's collapse, so the observed damage best correlates with the historic tsunami a few decades earlier in 115 CE. As the minimum size of this island was at least 25 m³, and as its concrete has an estimated minimum density of ~2400 kg/m³, its estimated weight should exceed 60 metric tons. Toppling such an island would have required significant force, and is analogous to damage that has been recorded to concrete harbor structures recently during the 2011 Tohoku-Oki tsunami in northern Japan events (Fig. 7, Ewing et al., 2013).

We hypothesize that the shallower subsurface reflector 'A' is the buried surface formed by backflow associated with the 8th century CE (possibly 749 CE) tsunami; this surface could also represent a composite with the 6th century CE (551 CE) event. We suggest that the multiple, distributed channels observed in that reflector's surface morphology (Fig. 6B) represent a complex back-channeling product produced by the less-organized/more degraded character of the harbor at that time. The Byzantine Era (4th–7th c. CE) was a busy time for Caesarea commercially, but with the exception of a 500 CE renovation, the harbor consisted primarily of the intermediate harbor (Fig. 1D) with very little, if any, surface presence of the outer harbor mole/jetty complex



Fig. 7. Photos of damaged cement harbor foundations at Kojirahama (Top left), Utuchi (middle), and Tanesashi (right), Japan following the March 11, 2010 Tohoku-Oki great earthquake (from Ewing, L.: from Lesley Ewing, Sr. Coastal Engineer California Coastal Commission, "Port & Harbor Damage from the March 11, 2011 Tohoku Oki Tsunami", www.coastal.ca.gov/nps/Tsunami_Lessons.pdf).

(Figs. 1D, 2; Reinhardt and Raban, 1999). Presuming that the map of reflector "A" gives us the ~post-8th century event state of the coastal sea bottom, the harbor would have been in an even more degraded condition through the early Islamic (7th–11th c. CE) period, with multiple disorganized approaches rather than a single cohesive entrance (Fig. 6B, right). Recently this chaotic character of the outer harbor at that time was reinforced with the discovery of thousands of gold coins dating to the 10–11th century that were presumably part of a shipwreck discovered on top of the submerged harbor in a depth of only 7.5 m, which could only be possible if that area was not a cohesive harbor at the time. Ship ballast concentrations and refuse have been recognized outside the harbor in a roughly shore-parallel, elongated oval shape that agrees with the pattern of debris that would be expected in an anchoring refuge for commercial transactions, given prevalent wind patterns and typical anchoring scope ratios (Boyce et al., 2009). This overlying refuse may be deposited immediately above the two tsunami horizons in question, suggesting that whatever condition the harbor was in prior to the 749/551 CE events, it was even more heavily compromised afterwards. As a result, by the 6th century CE, commercial ships likely had to anchor offshore as a standard practice.

Recently, in continuing efforts to link terrestrial archeological stratigraphy to the offshore sequence, evidence has been gathered to suggest that there are two distinct stratigraphic horizons with tsunamigenic features, one dating to the late Byzantine (~6th century CE) and the second to the early Islamic (8th century CE) periods (Fig. 4). Much of this evidence comprises of shell layers described in the terrestrial excavations that were previously interpreted as dredge debris (see Dey et al. 2014 for detailed discussion). However, thus far, only one offshore layer has been identified (Fig. 4). The original dating of that offshore horizon (Goodman-Tchernov et al., 2009; Fig. 4) was limited to a few sherds of ceramics that were ceramic types that remained in use over a long period that included the late Byzantine period and into the early Islamic era (~5–8th c. CE), and only one radiocarbon date has been obtained from shell material immediately above the horizon. After a more detailed review of the dating methods used for that horizon in previous studies, recent finds from shallow (<3 m) water excavations, and review of archeological reports from the hippodrome coastal area (Dey et al. 2014) we suggest that that the single horizon is actually the result of two separate tsunami events that occurred relatively close in time (~200 years), resulting in a single deposit. An upper date of 900–1050 CE (radiocarbon, Goodman-Tchernov et al., 2009) from the horizon immediately above the deposit, gives an upper limit for the tsunamite age, but also supports the possibility that both 6th and 8th century CE tsunami events contributed to the preserved horizon.

Following any tsunami event, sediments eroded and redeposited by the waves are exposed to later erosional and depositional processes. For Caesarea, the normal depositional regime, dominated by sandy sediments from the Nile River to the south, typically provides a positive

sediment budget necessary for burying the tsunamite. However, short intervals between tsunami events means that less inter-event sediment is available to bury and preserve the underlying tsunamites. **If a buried tsunamite is exposed and eroded during a later tsunami, then that material can be mixed and redeposited together with the later event, resulting in a single horizon.**

Evidence for such mixing offshore of Caesarea exists in multiple forms. First, archeological descriptions demonstrate the presence of tsunamigenic deposits on land south of the harbor, within the adjacent hippodrome area (see Figs. 1 and 2), of both 6th century A.D. and 8th century A.D. deposits (Dey and Goodman, 2010; Dey et al., 2014). In excavations of the shallow intermediate harbor (TN area, Fig. 1C; Reinhardt and Raban, 2008), there is an extensive deposit of mixed (Early Islamic-Byzantine-4th to 8th century CE) refuse, ranging from high-value intricate items of varying erosion state and exposure—suggesting broad mixing of typical harbor refuse (e.g., broken amphora/pots) and newly introduced, undamaged domestic wares and personal items (e.g., intricate hair combs, fine sections of Islamic coins, statuette, a satchel of copper coins). Unlike other harbor deposits, these materials are of broad origin (domestic, commercial, religious), value range and preservation state, suggesting the kind of non-deliberate and rapid burial a tsunami event would produce. In addition, because the ages of the ceramics found in this excavation range from early Islamic to late Byzantine (6th through 8th centuries CE), no distinctive stratigraphy offshore today separates what may have been two distinct tsunami events.

The expression of the different horizons in this offshore seismic survey is only possible due to the significant acoustic contrast in the physical properties between the tsunami event layers vs. the background, non-tsunami sediments (Fig. 5). **In the case of Caesarea, the background Nile River-derived sands are especially homogenous (siliciclastic, quartz-rich fine sands with a highly conservative mode value of ~169 μm), while the tsunamigenic layers consist of a range of grain sizes and inclusions of varying materials with far wider ranging physical properties (shell, broken kurkar cobbles, foreign ballast, pottery, etc.).** As a result, Caesarea may represent ideal conditions for the application of geophysical methods to tsunamite identification in the coastal zone. Other areas of the Mediterranean, and the world, where coasts with more meandering geomorphological features likely exhibit more variations and micro-environments in their natural background conditions, tsunamite definition is likely to be more problematic. Nonetheless, we feel that our results merit the effort to attempt similar merged mapping and archeological excavations/sampling elsewhere.

5. Conclusions

The results of the high-resolution seismic survey of Caesarea support previous studies that have argued for the presence of laterally extensive tsunamigenic deposits in and around that ancient harbor complex. Santorini-age tsunami deposits are present, but not everywhere

identifiable. The earlier interpretation that the ancient harbor of Caesarea was relatively intact at the time of the first historically documented tsunami that would have impacted it, ~1–2nd century, possibly 115 CE, is supported by the presence of pronounced (backwash) channels in association with the entrance to the ancient harbor. In contrast, the harbor's appearance was much degraded by the time of a known 8th century tsunami (749 CE), which is emphasized by the presence of a series of preserved remnant channels, testifying to multiple backwash paths. These preserved paleo-bathymetric features could be recognized at other archeological sites and may provide a new preserved indicator for ancient tsunamis, further reinforcing the usefulness of the offshore record, particularly relative to the relatively quickly altered and erased terrestrial record (Szczeniński, 2011).

Caesarea, an ancient urban harbor city with a concrete harbor comparable to many harbors of today, also provides insight into the effects of tsunamis on harbors and the nature of preserved deposits in and around them. We suggest that the intensification and magnification of tsunamis within harbors could provide an additional dataset for targeting and identifying non-documented tsunamis and improving the understanding of their impact on harbor structures, enhancing and expanding on the tsunami catalogues, as well as better understanding broader near and far-field effects elsewhere. A multitude of harbor sites both nearby (e.g., Tyre, Sidon, and Alexandria) and worldwide could contain these useful deposits.

Acknowledgments

Funding for this project was provided by a 2011 Innovation and Opportunity grant to JA from the Jackson School of Geosciences, The University of Texas/Austin, and Israel Science Foundation (894/10) and Israel Ministry of Energy and Water (29-17-041) grants to BNG, including private contributions by donors N. Kirscher, M. Davis, and T. Katz. We appreciate the useful conversations and proposal remarks provided by U. Schattner, Makovsky, M., Lazar. T. and Katz, S. Saustrup of UTIG processed the CHIRP profiles. L. Ewing (ASCE) assisted with photo acquisition. D. Meyer, R. Tsadok and other U of Haifa students contributed to the completion of the study during field course CCAP 2011, in close partnership with the Israel Antiquities Authority (K. Sharvit and D. Planar). UTIG Contribution No. — (#2851).

Appendix A. Supplementary data

Supplementary data to this article can be found online at <http://dx.doi.org/10.1016/j.jasrep.2015.06.032>.

References

- Amiran, R., Arieh, E., Turcotte, T., 1994. Earthquakes in Israel and Adjacent Areas : Observations. *Israel Exploration Journal* 44 (3), 260–305.
- Abrantes, F., Lebreiro, S., Rodrigues, T., Gil, I., Bartels-Jónsdóttir, H., Oliveira, P., Kissel, C., Grimalt, J.O., 2005. Shallow-marine sediment cores record climate variability and earthquake activity off Lisbon (Portugal) for the last 2000 years. *Quat. Sci. Rev.* 24 (23–24), 2477–2494. <http://dx.doi.org/10.1016/j.quascirev.2004.04.009>.
- Atwater, B.F., ten Brink, U.S., Buckley, M., Halley, R.S., Jaffe, B.E., López-Venegas, A.M., Reinhardt, E.G., Tuttle, M.P., Watt, S., Wei, Y., 2010. Geomorphic and stratigraphic evidence for an unusual tsunami or storm a few centuries ago at Anegada, British Virgin Islands. *Nat. Hazards* 63 (1), 51–84.
- Baird, A.H., Campbell, S.J., Anggoro, A.W., Ardiwijaya, R.L., Fadli, N., Herdiana, Y., Kartawijaya, T., Mahyiddin, D., Mukminin, A., Pardede, S.T., Pratchett, M.S., Rudi, E., Siregar, A.M., 2005. Acehnese reefs in the wake of the Asian tsunami. *Curr. Biol.* 15, 1926–1930.
- Bettwy, S.W., 2015. *Amphibious Warfare Since World War II*. Thomas Jefferson Sch. Law, SSRN-id2544746.
- Bourgeois, J., Hansen, T. a, Wiberg, P.L., Kauffman, E.G., 1988. A tsunami deposit at the cretaceous-tertiary boundary in Texas. *Science* 241, 567–570.
- Boyce, J.L., Reinhardt, E.G., Pozza, M.R., 2004. Marine magnetic survey of a submerged Roman harbour. *Int. J. Naut. Archaeol.* 33, 122–136.
- Boyce, J.L., Reinhardt, E.G., Goodman, B.N., 2009. Magnetic detection of ship ballast deposits and anchorage sites in King Herod's Roman harbour, Caesarea Maritima, Israel. *J. Archaeol. Sci.* 36, 1516–1526.

- Brandon, C., 1996. Cements, concrete, and settling barges at Sebastos: comparisons with other Roman harbour examples and the descriptions of Vitruvius. In: Raban, A., Holum, K.G. (Eds.), *Caesarea Maritima: A Retrospective After Two Millennia*. Brill, New York, pp. 25–40.
- Bruins, H.J., MacGillivray, J.A., Synolakis, C.E., Benjamini, C., Keller, J., Kisch, H.J., Klügel, A., van der Plicht, J., 2008. Geoarchaeological tsunami deposits at Palaikastro (Crete) and the Late Minoan IA eruption of Santorini. *J. Archaeol. Sci.* 35, 191–212.
- De Martini, P.M., Barbano, M.S., Smedile, a., Gerardi, F., Pantosti, D., Del Carlo, P., Pirrotta, C., 2010. A unique 4000 year long geological record of multiple tsunami inundations in the Augusta Bay (eastern Sicily, Italy). *Mar. Geol.* 276, 42–57.
- Dey, H., Goodman-Tchernov, B., Sharvit, J., 2014. Archaeological evidence for the tsunami of January 18, 749 Islamic: a chapter in the history of Early Caesarea, Qaysariyah (Caesarea Maritima). *Journal of Roman Archaeology* 27, 357–373.
- Dey, H.W., Goodman-Tchernov, B., 2010. Mediterranean Tsunamis and the Port of Caesarea Maritima over the Longue Durée: A Geoarchaeological Perspective. *Journal of Roman Archaeology* 23, 265–284.
- Ewing, L., Takahashi, S., Petroff, C., 2013. Tohoku, Japan, Earthquake and Tsunami of 2011. American Society of Civil Engineers, Reston, VA.
- Feldens, P., Schwarzer, K., Szczeniński, W., Statteger, K., 2009. Impact of 2004 Tsunami on Seafloor Morphology and Offshore Sediments, Pakarang Cape, Thailand 18. pp. 63–68.
- Fernando, H.J.S., McCulley, J.L., Mendis, S.G., Perera, K., 2005. Coral poaching worsens tsunami destruction in Sri Lanka. *EOS Trans. Am. Geophys. Union* 86, 301.
- Friedrich, W.L., Kromer, B., Friedrich, M., Heinemeier, J., Pfeiffer, T., Talamo, S., 2006. Santorini eruption radiocarbon dated to 1627–1600 B.C. *Science* 312, 548.
- Fritz, H.M., Petroff, C.M., Catalán, P.a., Cienfuegos, R., Winckler, P., Kalligeris, N., Weiss, R., Barrientos, S.E., Meneses, G., Valderas-Bermejo, C., Ebeling, C., Papadopoulos, A., Contreras, M., Almar, R., Dominguez, J.C., Synolakis, C.E., 2011. Field Survey of the 27 February 2010 Chile Tsunami. *Pure Appl. Geophys.* 168, 1989–2010.
- Galili, E., Horwitz, L.K., Hershkovitz, I., Eshed, V., Salamon, A., Zviely, D., Weinstein-Evron, M., Greenfield, H., 2008. Comment on "Holocene tsunamis from Mount Etna and the fate of Israeli Neolithic communities" by Maria Teresa Pareschi, Enzo Boschi, and Massimiliano Favalli. *Geophys. Res. Lett.* 35, 10–12.
- Giri, C., Zhu, Z., Tieszen, L.L., Singh, A., Gillette, S., Kelmelis, J.A., 2008. Mangrove forest distributions and dynamics (1975–2005) of the tsunami-affected region of Asia. *J. Biogeogr.* 35, 519–528.
- Goff, J., Chagué-Goff, C., Nichol, S., Jaffe, B., Dominey-Howes, D., 2012. Progress in palaeotsunami research. *Sediment. Geol.* 243–244, 70–88.
- Goldsmith, V., Golik, A., 1980. Sediment Transport Model of the Southeastern Mediterranean Coast. *Mar. Geol.* 37, 147–175.
- Goodman-Tchernov, B.N., Dey, H.W., Reinhardt, E.G., McCoy, F., Mart, Y., 2009. Tsunami waves generated by the Santorini eruption reached Eastern Mediterranean shores. *Geology* 37, 943–946.
- Goto, K., Chagué-Goff, C., Fujino, S., Goff, J., Jaffe, B., Nishimura, Y., Richmond, B., Sugawara, D., Szczeniński, W., Tappin, D.R., Witter, R.C., Yulianto, E., 2011a. New insights of tsunami hazard from the 2011 Tohoku-oki event. *Mar. Geol.* 290, 46–50.
- Goto, K., Takahashi, J., Oie, T., Imamura, F., 2011b. Remarkable bathymetric change in the nearshore zone by the 2004 Indian Ocean tsunami: Kirinda Harbor, Sri Lanka. *Geomorphology* 127, 107–116.
- Goto, K., Hashimoto, K., Sugawara, D., Yanagisawa, H., Abe, T., 2014. Spatial thickness variability of the 2011 Tohoku-oki tsunami deposits along the coastline of Sendai Bay. *Mar. Geol.* 358, 38–48. <http://dx.doi.org/10.1016/j.margeo.2013.12.015>.
- Griffin, W., 1984. *Crescent City's Dark Disaster*. Crescent City Printing Co., Crescent City, CA.
- Hohlfelder, R., 1996. Caesarea's master harbor builders: Lessons learned, lessons applied. In: Raban, A., Holum, K. (Eds.), *Caesarea Maritima: A Retrospective After Two Millennia*. Brill, pp. 77–101.
- Hohlfelder, R.L., Brandon, C., Oleson, J.P., 2007. Constructing the Harbour of Caesarea Palaestina, Israel: new evidence from the ROMACONS field campaign of October 2005. *Int. J. Naut. Archaeol.* 36, 409–415.
- Hohlfelder, R., 2000. Anastasius I, mud and foraminifera: conflicting views of Caesarea Maritima's harbour in late antiquity. *BASOR* 317, 41–62.
- Hohlfelder, R.L., 1988. Procopius, De Aedificiis 1.11.18–20: Caesarea Maritima and the building of Harbours in Late Antiquity. *Mediterr. Hist. Rev.* 3, 54–62.
- Holum, K., Hohlfelder, R.L., Bull, R., Raban, A., 1988. King Herod's Dream: Caesarea on the Sea. W W Norton Co., Inc, New York 244 pages.
- Hori, K., Kuzumoto, R., Hirouchi, D., Umitsu, M., Janjirawuttikul, N., Patanakanog, B., 2007. Horizontal and vertical variation of 2004 Indian tsunami deposits: an example of two transects along the western coast of Thailand. *Mar. Geol.* 239, 163–172.
- Horrillo, J., Knight, W., Kowalik, Z., 2008. Kuril Islands tsunami of November 2006: 2. Impact at Crescent City by local enhancement. *J. Geophys. Res.* 113, 1–12.
- Jackson, M., Vola, G., Všianský, D., Oleson, J., Scheetz, B., Brandon, C., Hohlfelder, R., 2012. Cement microstructures and durability in ancient Roman seawater concretes. In: Válek, J., Hughes, J.J., Groot, C.J.W.P. (Eds.), *Historic Mortars SE — 5*. RILEM Bookseries, Springer Netherlands, pp. 49–76.
- Jaffe, B.E., Goto, K., Sugawara, D., Richmond, B.M., Fujino, S., Nishimura, Y., 2012. Flow speed estimated by inverse modeling of sandy tsunami deposits: results from the 11 March 2011 tsunami on the coastal plain near the Sendai Airport, Yuriage Sendai Airport transect Area in Fig. 4. *Sediment. Geol.* 282, 90–109.
- Kaushik, H.B., Jain, S.K., 2007. Impact of Great December 26, 2004 Sumatra Earthquake and Tsunami on Structures in Port Blair. *J. Perform. Constr. Facil.* 21, 128–142.
- Kowalik, Z., Horrillo, J., Knight, W., Logan, T., 2008. Kuril Islands tsunami of November 2006: 1. Impact at Crescent City by distant scattering. *J. Geophys. Res. Oceans* 113, 1–11.

- Kunkel, C.M., Hallberg, R.W., Oppenheimer, M., 2006. Coral reefs reduce tsunami impact in model simulations. *Geophys. Res. Lett.* 33, 4–7.
- Lynett, P.J., Borrero, J.C., Weiss, R., Son, S., Greer, D., Renteria, W., 2012. Observations and modeling of tsunami-induced currents in ports and harbors. *Earth Planet. Sci. Lett.* 327–328, 68–74.
- Marco, S., Katz, O., Dray, Y., 2014. Historical sand injections on the Mediterranean shore of Israel: evidence for liquefaction hazard. *Nat. Hazards* p. 1449–1459.
- Mart, Y., Perelman, I., 1996. Neotectonic activity in Caesarea, the Mediterranean coast of central Israel. *Tectonophysics* 254, 139–153 <http://dx.doi.org/10.1007/s11069-014-1249-6>.
- Morhange, C., Salamon, A., Bony, G., Flaux, C., Galili, E., Goiran, J., Zviely, D., 2014. Geoarchaeology of tsunamis and the revival of neocatastrophism. *Rosapat* 11, 61–81.
- Mori, N., Takahashi, T., Yasuda, T., Yanagisawa, H., 2011. Survey of 2011 Tohoku earthquake tsunami inundation and run-up. *Geophys. Res. Lett.* 38, 1–6.
- Morton, R.A., Gelfenbaum, G., Jaffe, B.E., 2007. Physical criteria for distinguishing sandy tsunami and storm deposits using modern examples. *Sediment. Geol.* 200, 184–207.
- Neev, D., Bakler, N., Emery, K.O., 1987. *Mediterranean Coasts of Israel and Sinai: Holocene Tectonism From Geology, Geophysics, and Archaeology*. Taylor and Francis, New York.
- Neev, D., Emery, K.O., 1989. Coastal Landscape, in Raban, A. (Ed.), *The harbours of Caesarea Maritima: Results of the Caesarea Ancient Harbour Excavation Project*. British Archaeological Reports S491, Oxford, pp. 7–12.
- Okal, E.A., Fritz, H.M., Raad, P.E., Synolakis, C., Al-Shijbi, Y., Al-Saifi, M., 2006. Oman Field Survey after the December 2004 Indian Ocean Tsunami. *Earthq. Spectra* 22, 203–218.
- Okal, E.A., Synolakis, C.E., Uslu, B., Kalligeris, N., Voukouvalas, E., 2009. The 1956 earthquake and tsunamis in Amorgos, Greece. *Geophys. J. Int.* 178, 1533–1554.
- Papadopoulos, G.A., Gracia, E., Urgeles, R., Sallares, V., De Martini, P.M., Pantosti, D., González, M., Yalciner, A.C., Mascle, J., Sakellariou, D., Salamon, A., Tinti, S., Karastathis, V., Fokaefs, A., Camerlenghi, A., Novikova, T., Papageorgiou, A., 2014. Historical and pre-historical tsunamis in the Mediterranean and its connected seas: geological signatures, generation mechanisms and coastal impacts. *Mar. Geol.* 354, 81–109.
- Pareschi, M.T., Boschi, E., Favalli, M., 2007. Holocene tsunamis from Mount Etna and the fate of Israeli Neolithic communities. *Geophys. Res. Lett.* 34, 1–6.
- Paris, R., Wassmer, P., Sartohadi, J., Lavigne, F., Barthomeuf, B., Desgages, E., Grancher, D., Baumert, P., Vautier, F., Brunstein, D., Gomez, C., 2009. Tsunamis as geomorphic crises: Lessons from the December 26, 2004 tsunami in Lhok Nga, West Banda Aceh (Sumatra, Indonesia). *Geomorphology* v. 104 (1–2), p. 59–72. <http://dx.doi.org/10.1016/j.geomorph.2008.05.040>.
- Pilarczyk, J.E., Reinhardt, E.G., 2012. Testing foraminiferal taphonomy as a tsunami indicator in a shallow arid system lagoon: Sur, Sultanate of Oman. *Mar. Geol.* 295–298 (1851), 128–136. <http://dx.doi.org/10.1016/j.margeo.2011.12.002>.
- Pilarczyk, J.E., Horton, B.P., Witter, R.C., Vane, C.H., Chagué-Goff, C., Goff, J., 2012. Sedimentary and foraminiferal evidence of the 2011 Tōhoku-oki tsunami on the Sendai coastal plain, Japan. *Sediment. Geol.* 282, 78–89. <http://dx.doi.org/10.1016/j.sedgeo.2012.08.011>.
- Raban, A., 1992. Sebastos: the royal harbour at Caesarea Maritima—a short-lived giant. *Int. J. Naut. Archaeol.* 21, 111–124.
- Raban, A., 1995. The heritage of ancient harbour engineering in Cyprus and the Levant. In: Karageorghis, V., Michaelides, D. (Eds.), *Proceedings of the International Symposium "Cyprus and the Sea"*. University of Cyprus, Nicosia, pp. 167–168.
- Raban, A., 2008. Underwater excavations in the Herodian harbor Sebastos, 1995–1999 seasons. In: Holum, K., Stabler, J., Reinhardt, E. (Eds.), *Caesarea Reports and Studies: Excavations 1995–2007*, pp. 129–142.
- Raban, A., 2009. *The Harbour of Sebastos (Caesarea Maritima) in its Roman Mediterranean Context*. BAR International Series 1930, Oxford.
- Raichlen, F., 1966. Harbor resonance. In: Ippen, A.T. (Ed.), *Coastline and Estuarine Hydrodynamics*. McGraw-Hill, New York, pp. 281–340.
- Reinhardt, E., Raban, A., 1999. Destruction of Herod the Great's harbor at Caesarea Maritima, Israel — geoarchaeological evidence. *Geology* 27, 811–814.
- Reinhardt, E., Raban, A., 2008. Site formation and stratigraphic development of Caesarea's ancient harbor. In: Holum, K., Stabler, J., Reinhardt, E.G. (Eds.), *Caesarea Reports and Studies: Excavations 1995–2007*, pp. 155–182.
- Reinhardt, E.G., Patterson, R.T., Schroeder-Adams, C.J., 1994. Geoarchaeology of the ancient harbor site of Caesarea Maritima, Israel; evidence from sedimentology and paleoecology of benthic foraminifera. *J. Foraminif. Res.* 24, 37–48.
- Reinhardt, E.G., Goodman, B.N., Boyce, J.I., Lopez, G., van Hengstum, P., Rink, W.J., Mart, Y., Raban, A., 2006. The tsunami of 13 December A.D. 115 and the destruction of Herod the Great's harbor at Caesarea Maritima, Israel. *Geology* 34, 1061.
- Rhodes, B., Tuttle, M., Horton, B., Doner, L., Kelsey, H., Nelson, A., Cisternas, M., 2006. Paleotsunami Research. *EOS Trans. Am. Geophys. Union* 87, 205–209.
- Richmond, B., Szczucinski, W., Chagué-Goff, C., Goto, K., Sugawara, D., Witter, R., Tappin, D.R., Jaffe, B., Fujino, S., Nishimura, Y., Goff, J., 2012. Erosion, deposition and landscape change on the Sendai coastal plain, Japan, resulting from the March 11, 2011 Tohoku-oki tsunami. *Sediment. Geol.* 282, 27–39.
- Rothaus, R.M., Reinhardt, E., Noller, J., 2004. Regional considerations of coastline change, tsunami damage and recovery along the Southern Coast of the Bay of Izmit (The Kocaeli (Turkey) Earthquake of 17 August 1999). *Nat. Hazards* 31, 233–252.
- Ryan, C., 1959. *The Longest Day: June 6, 1944*. Simon and Schuster, New York.
- Shalem, N., 1956. *Sismic Tidal Waves (Tsunamis) in the eastern Mediterranean*. Israel Exploration Society p. 159–72.
- Sivan, D., Porat, N., 2004. Evidence from luminescence for Late Pleistocene formation of calcareous aeolianite (kurkar) and paleosol (hamra) in the Carmel Coast, Israel. *Palaeogeogr. Palaeoclimatol. Palaeoecol.* 211, 95–106.
- Smedile, A., De Martini, P.M., Pantosti, D., 2012. Combining inland and offshore paleotsunamis evidence: the Augusta Bay (eastern Sicily, Italy) case study. *Nat. Hazards Earth Syst. Sci.* 12, 2557–2567.
- Stanford, A.B., 1951. *The Planning and Installation of the Artificial Harbor Off U.S. Normandy Beaches in World War II*. William Morrow and Co., Morrow, New York.
- Stanley, D.J., 1989. Sediment transport on the coast and shelf between the Nile Delta and Israeli Margin as determined by heavy minerals. *J. Coast. Res.* 5, 813–828.
- Sugawara, D., Imamura, F., Goto, K., Matsumoto, H., Minoura, K., 2012. The 2011 Tohoku-oki Earthquake Tsunami: similarities and differences to the 869 Jogan Tsunami on the Sendai Plain. *Pure Appl. Geophys.* 170, 831–843.
- Synolakis, C.E., Okal, E.A., 2005. 1992–2002: perspective on a decade of post-tsunami surveys, in Tsunamis: case studies and recent developments. In: Satake, K. (Ed.), *Advances Nature Technology Hazards*. Springer, Dordrecht, pp. 1–30.
- Szczuciński, W., 2011. The post-depositional changes of the onshore 2004 tsunami deposits on the Andaman Sea coast of Thailand. *Nat. Hazards* 60 (1), 115–133. <http://dx.doi.org/10.1007/s11069-011-9956-8>.
- Umitsu, M., Tanavud, C., Patanakanog, B., 2007. Effects of landforms on tsunami flow in the plains of Banda Aceh, Indonesia, and Nam Khem, Thailand. *Mar. Geol.* 242, 141–153.
- Vandenbergh, G., Boer, W., Dehaas, H., Vanweering, T., Vanwijhe, R., 2003. Shallow marine tsunami deposits in Teluk Banten (NW Java, Indonesia), generated by the 1883 Krakatau eruption. *Mar. Geol.* 197, 13–34.
- Votruba, G.F., 2007. Imported building materials of Sebastos Harbour, Israel. *Int. J. Naut. Archaeol.* 36, 325–335.
- Vött, A., 2011. Tsunamis – Entstehung, Dynamik, Ausmaß und Überlieferung. In: Gebhardt, H., Glaser, R., Radtke, U., Reuber, P. (Eds.), *Geographie. Physische Geographie und Humangeographie*, 2nd edition Spektrum Akademischer Verlag, Berlin, Heidelberg, pp. 1134–1137.
- Vött, A., Brückner, H., Brockmüller, S., Handl, M., May, S.M., Gaki-Papanastassiou, K., Herd, R., Lang, F., Maroukian, H., Nelle, O., Papanastassiou, D., 2009. Traces of Holocene tsunamis across the Sound of Lefkada, NW Greece. *Glob. Planet. Chang.* 66, 112–128.
- Weiss, R., Bahlburg, H., 2006. A note on the preservation of offshore tsunami deposits. *J. Sediment. Res.* 76, 1267–1273.
- Wilson, R.L., Admire, A.R., Borrero, J.C., Dengler, L.A., Legg, M.R., Lynett, P., McCrink, T.P., Miller, K.M., Ritchie, A., Sterling, K., Whitmore, P.M., 2013. Observations and impacts from the 2010 Chilean and 2011 Japanese Tsunamis in California (USA). *Pure Appl. Geophys.* 170, 1127–1147.
- Yawsangratt, S., Szczuciński, W., Chaimanee, N., Chatprasert, S., Majewski, W., Lorenc, S., 2011. Evidence of probable paleotsunami deposits on Kho Khao Island, Phang Nga Province, Thailand. *Nat. Hazards* 63, 151–163.
- Zviely, D., Kit, E., Klein, M., 2007. Longshore sand transport estimates along the Mediterranean coast of Israel in the Holocene. *Mar. Geol.* 238, 61–73.